2015

Large-scale synthesis of ordered mesoporous carbon fiber and its application as cathode material for lithium-sulfur batteries

Hongqiang Wang
University of Wollongong, hw571@uowmail.edu.au

Chaofeng Zhang
University of Wollongong, czhang@uow.edu.au

Zhixin Chen
University of Wollongong, zchen@uow.edu.au

Hua-Kun Liu
University of Wollongong, hua@uow.edu.au

Zaiping Guo
University of Wollongong, zguo@uow.edu.au

Large-scale synthesis of ordered mesoporous carbon fiber and its application as cathode material for lithium-sulfur batteries

Abstract

A novel type of one-dimensional ordered mesoporous carbon fiber has been prepared via the electrospinning technique by using resol as the carbon source and triblock copolymer Pluronic F127 as the template. Sulfur is then encapsulated in this ordered mesoporous carbon fibers by a simple thermal treatment. The interwoven fibrous nanostructure has favorably mechanical stability and can provide an effective conductive network for sulfur and polysulfides during cycling. The ordered mesopores can also restrain the diffusion of long-chain polysulfides. The resulting ordered mesoporous carbon fiber sulfur (OMCF-S) composite with 63% S exhibits high reversible capacity, good capacity retention and enhanced rate capacity when used as cathode in rechargeable lithium-sulfur batteries. The resulting OMCF-S electrode maintains a stable discharge capacity of 690 mAh/g at 0.3 C, even after 300 cycles.

Disciplines

Engineering | Physical Sciences and Mathematics

Large-scale synthesis of ordered mesoporous carbon fiber and its application as cathode material for lithium-sulfur batteries

Hongqiang Wang [a], Chaofeng Zhang [a], Zhixin Chen [c], Hua Kun Liu [a], Zaiping Guo[a,b,c,*]

[a] Institute for Superconducting & Electronic Materials, University of Wollongong, NSW 2522, Australia

[b] Hubei Collaborative Innovation Center for Advanced Organic Chemical Materials, College of Chemistry and Chemical Engineering, Hubei University, Wuhan 430062, P.R. China

[c] School of Mechanical, Materials & Mechatronics Engineering, University of Wollongong, NSW 2500, Australia.

ABSTRACT:

A novel type of one-dimensional ordered mesoporous carbon fiber has been prepared via the electrospinning technique by using resol as the carbon source and triblock copolymer Pluronic F127 as the template. Sulfur is then encapsulated in this ordered mesoporous carbon fibers by a simple thermal treatment. The interwoven fibrous nanostructure has favorably mechanical stability and can provide an effective conductive network for sulfur and polysulfides during cycling. The ordered mesopores can also restrain the diffusion of long-chain polysulfides. The resulting ordered mesoporous carbon fiber sulfur (OMCF-S) composite with 63% S exhibits high reversible capacity, good capacity retention and enhanced rate capacity when used as cathode in rechargeable lithium-sulfur batteries. The resulting OMCF-S electrode maintains a stable discharge capacity of 690 mAh/g at 0.3 C, even after 300 cycles.

1. Introduction

Due to its ultra-high energy density (theoretically 2567 Wh kg^{-1}) and high theoretical specific capacity (1675 mAh·g^{-1}), the rechargeable lithium-sulfur (Li-S) battery has attracted enormous attention in the last several years [1-3]. Sulfur cathodes face several major challenges, however, which limit their practical applications, including the low conductivity of sulfur and lithium sulfide [4,5], as well as the large volume changes in the sulfur particles during charge and discharge processes. A more significant challenge that needs to be

---

* Corresponding author. E-mail: zguo@uow.edu.au (Zaiping Guo)

overcome is the high solubility of high-order polysulfide intermediates in organic electrolytes. The dissolved high-order polysulfides can diffuse from the cathode and react with the lithium anode either to generate insoluble lower-order polysulfides in the form of Li_2S or Li_2S_2, leading to the precipitation of these species on the surface during cyclic processes, or form soluble low-order polysulfides, which is then transported back to the cathode side, resulting in a shuttle reaction [6,7]. The shuttle reaction and deposition of Li_2S or Li_2S_2 on the Li anode lead to the low utilization of sulfur, low coulombic efficiency of the sulfur cathode, and fast capacity fading [8,9].

There are two basic strategies to address this problem. The major stream of Li-S research has focused on the design "inside" the cathode, confining sulfur within various kinds of porous matrixes, such as porous carbon [10-16] or graphene [17-19], or applying surface coatings of conductive polymer [20-21] or metal oxides such as TiO_2 [22] or Al_2O_3 [23] to act as a physical barrier to prevent the soluble polysulfides from dissolving in the organic electrolyte. An alternative route has concentrated on the "outside" of the cathode, such as by modification of the electrolyte [24-26] and novel cell configurations [27-29].

Herein, we report a simple electrospinning deposition method (ESD), which can mass-produce ordered mesoporous carbon fiber (OMCF). Currently, the majority of carbon materials used for confining sulfur so far are difficult to be applied in practical applications due to their complicated preparation processing and high cost. The ESD method is considered a promising method to mass-produce one-dimensional (1D) carbon materials with the advantages of simplicity, efficiency, low cost, and high yield. We have employed 1D OMCF as an improved confinement matrix for high-level sulfur impregnation. The ordered mesoporous fibrous structure builds a framework of well-connected empty sites, which could encapsulate a large amount of sulfur. Furthermore, the OMCF framework could facilitate the transport of electrons and ions and the electrolyte diffusion, and retain the polysulfides, enhancing the reversibility of electrode, which is hardly achieved by random porous structures.

2. Experimental section

2.1 Synthesis of OMCF

The OMCF was synthesized through the electrospinning technique. In a typical synthetic process, 2 g F127 was put in 8 g of ethanol with 1.2 g 0.2 M HCl and stirred for 1 h at 40 °C to yield a transparent solution. Next, 6 g of 20 wt% resol ethanolic solution and 1.8 g tetraethyl orthosilicate (TEOS) were added in that order. The resol precursor ($M_w < 500$) was synthesized on the basis of previous report [30]. After being stirred for 5 h, 3g 25% polyvinyl butyral (PVB) solution in ethanol was added to the mixture. Finally, a homogeneous solution was obtained after 4 h strong mechanical stirring. Triblock copolymer Pluronic F127 and resol are regarded as template and carbon source, respectively. The role of PVB is to improve the "spinnability" of the solution, while the TEOS acts as a skeleton in the formation process for the mesoporous structure, which can be removed in the next step. The experimental procedure and the formation of ideal mesoporous structure of OMCF are shown in Fig. 1. During electrospinning process, the solution was
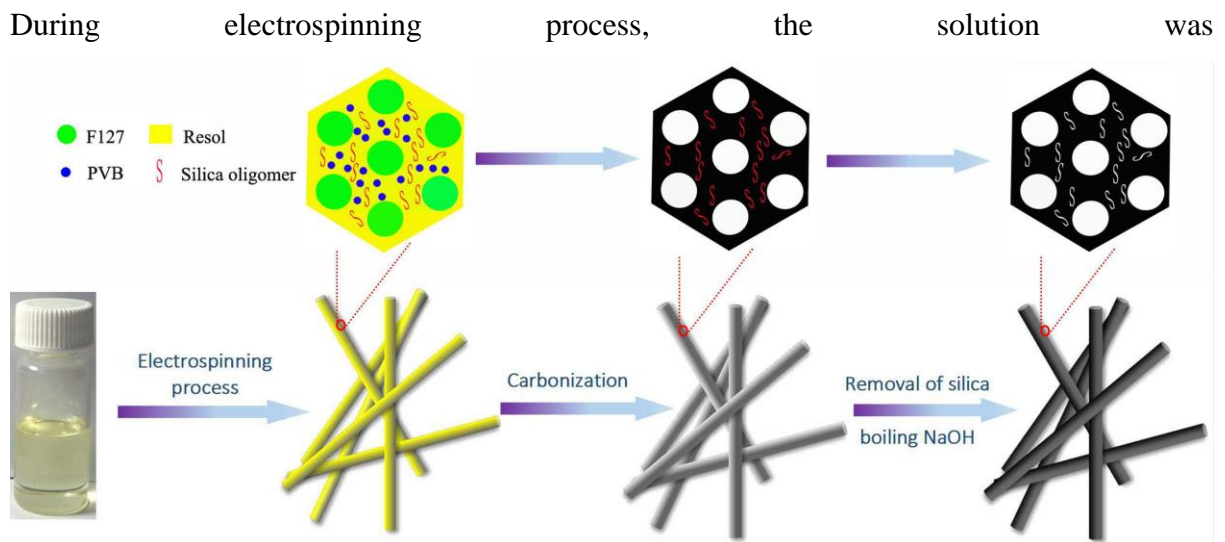

Fig. 1 A schematic illustration of the experimental procedure and the formation of ideal mesoporous structure of OMCF.

loaded into a syringe with a metallic needle (inner diameter 0.5 mm) and a flow rate of 0.8 mL h^{-1} under the voltage of 14.5 kV. The distance from needle tip to stainless steel mesh collector was 12 cm. Then, the collected primary film was dried at room temperature for 24 h. The as-prepared products were heat-treated at 700 °C for 2 h under flowing nitrogen gas. Afterwards, the resultant ordered mesoporous carbon–silica fiber was put into 2 mol/L boiling NaOH solution for 2 h to remove the silica to obtain OMCF. In our study, 0.2 g OMCF can be obtained per hour under our preparation condition, and the production can be

easily scale-up. The control sample ordered mesoporous carbon powder (OMCP) was synthesized through the same process as the OMCF, but without electrospinning technique.

2.2 Fabrication of ordered mesoporous carbon fiber sulfur (OMCF-S) composite

The as-prepared OMCF and OMCP were mixed with sulfur in a weight ratio of 25:75 and heated to 160 °C in a sealed stainless steel autoclave for 24 h to facilitate sulfur diffusion into the carbon host to obtain the OMCF-S and ordered mesoporous carbon powder sulfur (OMCP-S) composite, respectively. Then, the OMCF-S and OMCP-S composite was heated at 200 °C and kept for 10 minutes under flowing argon gas (50 cm^3s^{-1}) to vaporize the sulfur deposited on the outside surface of the composite.

2.3 Characterization

The crystal structures of the samples were carried out by powder X-ray diffraction (XRD, MMA GBC, Australia) and by Raman spectroscopy on an instrument (JOBIN YVON HR800) equipped with a 632.8 nm diode laser. Thermogravimetric analysis (TGA) was performed to measure the sulfur content with a METTLER TOLEDO TGA/DSC instrument with a heating rate of 10 °C min^{-1} from room temperature to 500 °C under a flow of argon. The specific surface areas and the pore size distribution were analyzed by Brunauer–Emmett–Teller (BET) method and Barrett–Joyner–Halenda (BJH) model, respectively. The morphologies of the samples were analyzed by JEOL JSM-7500FA field-emission scanning electron microscopy (FESEM), and by JEOL 2011 transmission electron microscopy (TEM).

2.4 Electrochemical measurement

To prepare the working electrodes, the OMCF-S and OMCP-S composite was mixed with carbon black, poly(ethylene oxide) (PEO), and poly(vinylpyrrolidone) (PVP) (75:15:8:2 by weight) in deionized water to form a slurry, respectively. The slurry was then coated onto aluminum foil and dried at 50 °C for 24 h. Coin-type (CR2032) cells were assembled by inserting a carbonized filter paper between cathode and the separator in an argon-filled glove box. The electrolyte used was 1 M lithium bis(trifluoromethanesulfonyl)imide in a solvent mixture of 1,3-dioxolane (DOL): dimethoxyethane (DME) (1:1, v/v) containing $LiNO_3$ (1 wt%). The cells were galvanostatically cycled from 1.8 to 2.6 V by using LAND CT2001A instrument.

3. Results and discussion

Fig. 2a presents SEM image of the resol/F127/TEOS/PVB precursor fibers before calcination. Obviously, the as-spun resol/F127/TEOS/PVB sample has good fibrous morphology with smooth surfaces and a uniform fiber diameter of less than 1 μm, indicating that the aqueous solution containing resol, PVB, and TEOS has excellent spinnability. From Fig. 2b, it is found that the OMCF after heat-treatment and the removal of the silica still maintains this
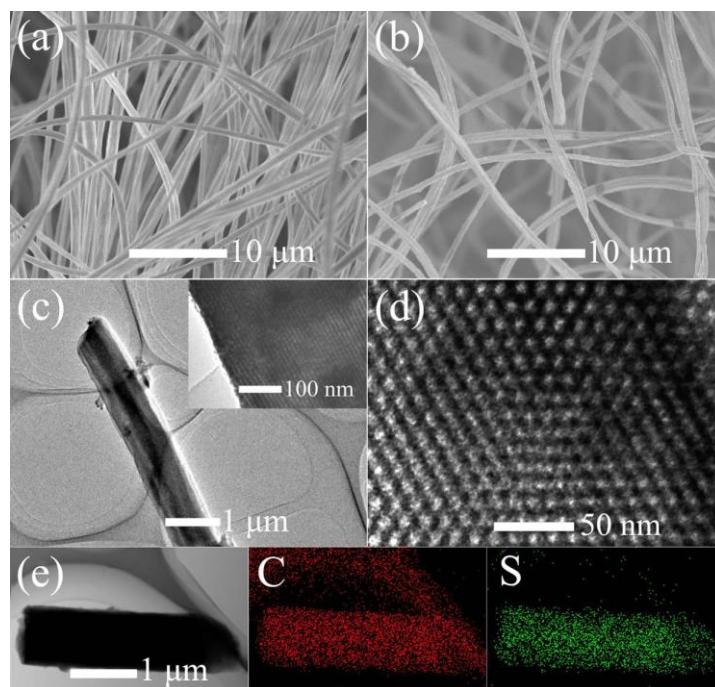

Fig. 2 SEM images of (a) electrospun resol/F127/TEOS/PVB fiber and (b) OMCF; TEM images of OMCF at (c) low magnification, with the inset and (d) showing high magnification; (e) STEM image of OMCF-S and corresponding elemental mapping images of C and S.

fibrous morphology, but exhibits a wrinkled surface morphology, mainly due to the large weight loss accompanied by gas evolution and removal of silica. The TEM characterizations of the OMCF were performed to further investigate the ordered mesopore structure (Fig. 2c and 2d). The OMCF shows ordered hexagonal mesostructure in large domains (mesopores with diameters of about 7 nm). The mesoporous structure is directly related to the battery performance of the sulfur cathode. Fig. 2e shows scanning TEM (STEM) and corresponding elemental mapping images of the OMCF-S composite, confirming that the sulfur is homogeneously distributed in the framework of the OMCF matrix.

The N_2 sorption isotherms in Fig. 3a illustrate the variation in the structural features of the OMCF before and after sulfur loading. The isotherms of the OMCF and OMCF-S are type IV isotherms with hysteresis at relative pressure above 0.4, which is characteristic of mesopores.
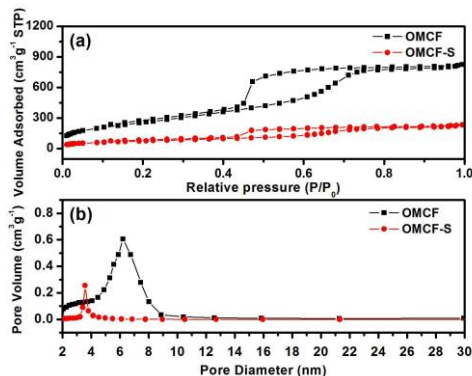

Fig. 3 (a) N_2 sorption isotherms and (b) pore-size distributions of the OMCF and OMCF-S composite.

The OMCF host exhibits a high specific surface area of 1345 m^2/g and a large pore volume of 1.21 cm^3/g. After the sulfur is embedded, the surface area and pore volume decrease to 335 m^2/g and 0.41 cm^3/g, respectively. Meanwhile, the pore size in Fig. 3b displays a strong decrease as well, from 6.2 nm to 3.5 nm. This indicates that a large proportion of the mesopores are filled with sulfur. The amount of sulfur in the OMCF-S composite is 63 wt% (Fig. S1).

The XRD patterns for the OMCF, S, and OMCF-S are shown in Fig. 4a. The low intensity
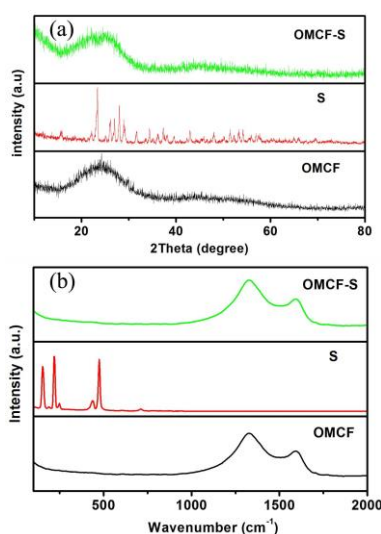

Fig. 4 (a) XRD patterns and (b) Raman spectra of the OMCF, S, and OMCF-S composite.
and the high peak broadening are typical feature of amorphous carbon in the OMCF sample.

No peaks corresponding to silica can be observed, suggesting that silica has been removed completely from the composite. In contrast, the pure elemental sulfur has well-defined diffraction peaks, corresponding to an orthorhombic structure. Although there is a substantial amount of sulfur (63%) in the OMCF-S composite, the signature peaks of elemental sulfur were not observed, indicating that the embedded sulfur in the composite exists in the form of small molecules and thus loses its characteristic of orthorhombic structure. This suggests good dispersion of the S within the porous carbon host [31]. Raman spectra of OMCF, S, and OMCF-S composite were also carried out to further observe their structure in Fig. 4b. Sulfur shows a series of typical Raman peaks which can be assigned to the S-S bond [32], however, such typical sulfur peaks disappeared in the OMCF-S, indicating that sulfur is successfully embedded into the pores of the OMCF.

Voltage profiles of the OMCF-S electrodes at various cycles are shown in Fig. 5a. The control sample OMCP-S powder was synthesized through the same process as the OMCF, but without electrospinning technique. The OMCP also shows ordered mesoporous structure with pore
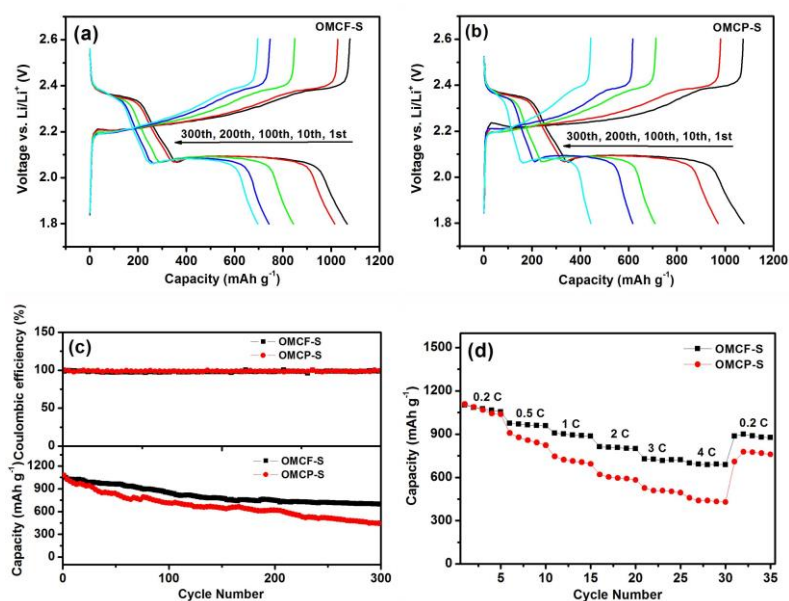

Fig. 5 Voltage profiles of (a) OMCF-S and (b) OMCP-S for selected cycles; (c) cycling performances of OMCF-S and OMCP-S electrodes at 0.3 C; (d) rate capabilities of OMCF-S and OMCP-S electrodes.

size of about 7 nm (Fig. S2 and S3). The upper plateau at 2.3 V corresponds to the reduction of sulfur (S_8) to soluble lithium polysulfides (Li_2S_4), and the lower plateau at 2.1 V represents the further reduction of polysulfides to Li_2S_2 or Li_2S [3,19,33]. The discharge plateau of the

OMCP-S composite electrode (in Fig. 5b) obviously shrinks with increased cycle number, however, the OMCF-S electrode has a good overlap of discharge plateaus during the cycling tests, suggesting the excellent stability and reversibility of the OMCF-S electrode. Fig. 5c displays the cycling performances of the OMCF-S and OMCP-S electrodes. The initial discharge capacities for the OMCF-S and OMCP-S electrodes were 1070 and 1080 mAh/g at 0.3 C, respectively. After 300 cycles, the OMCF-S electrodes retained a reversible capacity of 690 mAh/g, while only 450 mAh/g was left for the OMCP-S electrode. Even at the rate of 1 C, the OMCF-S electrodes can still maintain 570 mAh g^{-1} after 500 cycles (Fig. S4), indicating a superior cycling performance compared to that of OMCP-S electrodes. The rate capability of the OMCF-S and OMCP-S electrodes is displayed in Fig. 5d. The discharge capacity gradually reduced with the increase of rate from 0.2 C to 4 C. The OMCF-S electrode delivered a satisfactory capacity of 700 mAh/g, even at 4 C, but only a capacity of 440 mAh g^{-1} was obtained for OMCP-S electrode. The 1D interwoven fibrous mesoporous nanostructure with small dimension and large surface area can provide an effective conductive network for sulfur and polysulfides and facilitate the efficient contact between active materials and electrolyte. The ordered mesoporous structure can also effectively restrain the diffusion of long-chain polysulfides during cycling process. In addition, 1D architecture also possesses favorably structure stability, which can help to alleviate the structure damage caused by volume expansion and to keep the integrity of the electrodes during the cycling process especially for long cycles. All these features result in such a good cycling and rate capabilities performance. Fig. 6a shows the CV profiles of the OMCF-S cell in the voltage range of 1.8-2.6 V with a
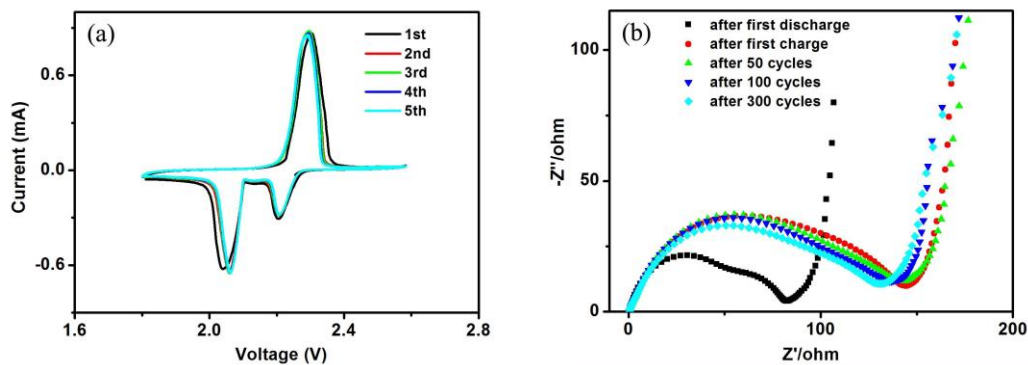

Fig. 6 (a) CV curves of the OMCF-S electrode before cycling; (b) EIS spectra of the OMCF-S electrodes after cycles.

scanning rate of 0.2 mV s^{-1}. Typical reduction and oxidation peaks representing for reaction of sulfur with lithium during the charge-discharge processes can be observed [19,34]. The sharp redox peaks with stable overlapping features confirm the high reversibility and excellent stability of electrode after first cycle [20,35]. The electrochemical impedance spectroscopy (EIS) analysis for the OMCF-S electrode was also carried out are shown in Fig. 6b. All the EIS curves show a semicircular loop whose diameter represents the charge-transfer resistance. The semicircle at high frequency is associated with the charge transfer resistance (R_{ct}) of the sulfur electrode, which is mainly generated at the interface between the electrode and the electrolyte [36,37]. The electrolyte resistance R_{ct} remained unchanged even after 300 cycles, indicating that polysulfides were well constrained in the cathode and to the dissolution of polysulfides into electrolyte and the increase of viscosity were successfully avoided. The R_{ct} is stabilized at around 150 Ω cm^2 (calculated after the electrode area normalization) after the first cycle, suggesting a stable electrochemical environment in the batteries.

To further investigate the reason why the OMCF-S electrode shows enhanced performance of the lithium-sulfur battery compared to OMCP-S electrode, the microstructure of the OMCF-S
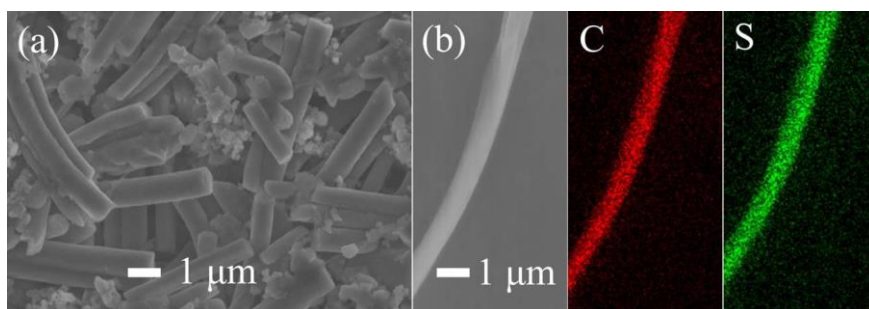

Fig. 7 SEM images of (a) OMCF-S electrode after 100 cycles, and (b) corresponding elemental map images of carbon, and sulfur.

electrode after 100 cycles for Li-S batteries was examined by SEM. The fibrous structure is still maintained is shown in the Fig. 7, and no obvious change is observed. The elemental mapping results show that sulfur is still homogeneously distributed throughout the whole fiber, suggesting the excellent mechanical stability of the OMCF-S, which makes a great

contribution to excellent electrochemical properties of OMCF-S electrode together with its ordered mesoporous structure.

4. Conclusions

In summary, ordered mesoporous carbon fibers were synthesized by the electrospinning technique and used to fabricate carbon-sulfur composite, which was then explored as a cathode material for lithium-sulfur batteries. Not only can the ordered mesoporous structure ensure good electrical pathways for the active sulfur, but it also can effectively trap soluble polysulfide intermediates during charge-discharge processes. In addition, the OMCF-S composite has excellent mechanical stability during charge-discharge process. All the features lead to excellent electrochemical performance for OMCF-S electrode (690 mAh/g even after 300 cycles). In particular, the OMCF can be mass produced in a simple way at low cost, which makes our sulfur-based electrode highly promising for practical application in lithium-sulfur batteries.

References

[1] Cheon SE, Choi SS, Han JS, Choi YS, Jung BH, Lim HS. Capacity fading mechanisms on cycling a high-capacity secondary sulfur cathode. J Electrochem Soc 2004;151(12):A2067-73.

[2] Bruce PG, Freunberger SA, Hardwick LJ, Tarascon JM. Li–O_2 and Li–S batteries with high energy storage. Nat Mater 2012;11(1):19-29.

[3]Shim J, Striebel KA, Cairns EJ. The lithium/sulfur rechargeable cell-effects of electrode composition and solvent on cell performance. J Electrochem Soc 2002;149(10):A1321-5.

[4] Novak P, Muller K, Santhanam KSV, Haas O. Electrochemically active polymers for rechargeble batteries. Chem Rev 1997;97(1):207-81.

[5] Yang Y, Zheng GY, Misra S, Nelson J, Toney MF, Cui Y. High-capacity micrometer-sized Li_2S particles as cathode materials for advanced rechargeable lithium-ion batteries. J Am Chem Soc 2012;134(37):15387-94.

[6] Mikhaylik YV, Akridge JR. Polysulfide shuttle study in the Li/S battery system. J Electrochem Soc 2004;151(11):A1969-76.

[7] Ahn W, Kim KB, Jung KN, Shin KH, Jin CS. Synthesis and electrochemical properties of a sulfur-multi walled carbon nanotubes composite as a cathode material for lithium sulfur batteries. J Power Sources 2012;202:394-9.

[8] Wang HL, Yang Y, Liang YY, Robinson JT, Li YG, Jackson A, et al. Graphene-wrapped sulfur particles as a rechargeable lithium-sulfur battery cathode material with high capacity and cycling stability. Nano Lett 2011;11(7):2644-7.

[9] Ellis BL, Lee KT, Nazar LF. Positive electrode materials for Li-ion and Li-batteries. Chem Mater 2010;22(3):691-714.

[10] Guo JC, Xu YH, Wang CS. Sulfur-impregnated disordered carbon nanotubes cathode for lithium-sulfur batteries. Nano Lett 2011;11(10):4288-94.

[11] Wu HB, Wei SY, Zhang L, Xu R, Hng HH, Lou XW. Embedding sulfur in MOF-derived microporous carbon polyhedrons for lithium-sulfur batteries. Chem Eur J 2013;19(33):10804-8.

[12] Lee BS, Son SB, Park KM, Lee G, Oh KH, Lee SH, et al. Effect of pores in hollow carbon nanofibers on their negative electrode properties for a lithium rechargeable battery. ACS Appl Mater Inter 2012;4(12):6701-9.

[13] Zhang CF, Wu HB, Yuan CZ, Guo ZP, Lou XW. Confining sulfur in double-shelled hollow carbon spheres for lithium-sulfur batteries. Angew Chem Int Ed 2012;51(38):9592-5.

[14] Zheng SY, Chen Y, Xu YH, Yi F, Zhu YJ, Liu YH, et al. In situ formed lithium sulfide/microporous carbon cathodes for lithium-ion batteries. ACS Nano 2013;7(12):10995-1003.

[15] Park MS, Jeong BO, Kim TJ, Kim S, Kim KY, Yu JS, et al. Disordered mesoporous carbon as polysulfide reservoir for improved cyclic performance of lithium-sulfur batteries. Carbon 2014;68:265-72.

[16] Jayaprakash N, Shen J, Moganty SS, Corona A, Archer LA. Porous hollow carbon@sulfur composites for high-power lithium–sulfur batteries. Angew Chem Int Ed 2011;50(26):5904-8.

[17] Li NW, Zheng MB, Lu HL, Hu ZB, Shen CF, Chang XF, et al. High-rate lithium-sulfur batteries promoted by reduced graphene oxide coating. Chem Commun 2012;48(34):4106-8.

[18] Ji LW, Rao M, Zheng HM, Zhang L, Li YC, Duan WH, et al. Grapehene oxide as a sulfur immobilizer in high performance lithium/sulfur cells. J Am Chem Soc 2011;133(46):18522-5.

[19] Wang JZ, Lu L, Choucair M, Stride JA, Xu X, Liu HK. Sulfur-graphene composite for rechargeable lithium batteries. J Power Sources 2011;196(16):7030-4.

[20] Xiao LF, Cao YL, Xiao J, Schwenzer B, Engelhard MH, Saraf LV, et al. A soft approach to encapsulate sulfur: polyaniline nanotubes for lithium-sulfur batteries with long cycle life. Adv Mater 2012;24(9):1176-81.

[21] Yang Y, Yu GH, Cha JJ, Wu H, Vosgueritchian M, Yao Y, et al. Improving the performance of lithium-sulfur batteries by conductive polymer coating. ACS Nano 2011;5(11):9187-93.

[22] Seh ZW, Li WY, Cha JJ, Zheng GY, Yang Y, Mcdowell MT, et al. Sulphur-TiO_2 yolk-shell nanoarchitecture with internal void space for long-cycle lithium-sulphur batteries. Nat Commun 2013;4:1331.

[23] Kim H, Lee JT, Lee DC, Magasinski A, Cho WI, Yushin G. Plasma-enhanced atomic layer deposition of ultrathin oxide coating for stabilized lithium-sulfur batteries. Adv Energy Mater 2013;3(10):1308–15.

[24] Zhang SS, Tran DT. How a gel polymer electrolyte affects performance of lithium/sulfur batteries. Electrochim Acta 2013;114:296-302.

[25] Weng W, Pol VG, Amine K. Ultrasound assisted design of sulfur/carbon cathodes with partially fluorinated ether electrolytes for highly efficient Li/S batteries. Adv Mater 2013;25(11):1608-15.

[26] Azimi N, Weng W, Takoudis C, Zhang ZC. Improved performance of lithium-sulfur battery with fluorinated electrolyte. Electrochem Commun 2013;37:96-9.

[27] Su YS, Manthiram A. Lithium-sulfur batteries with a microporous carbon paper as a bifunctional interlayer. Nat Commun 2012;3:1166.

[28] Su YS, Manthiram A. A new approach to improve cycle performance of rechargeable lithium-sulfur batteries by inserting a free-standing NMCNT interlayer. Chem Commun 2012;48(70):8817-9.

[29] Han XG, Xu YH, Chen XY, Chen YC, Weadock N, Wan JY, et al. Reactivation of dissolved polysulfides in Li-S batteries based on atomic layer deposition of Al_2O_3 in nanoporous carbon cloth. Nano Energy 2013;2:1197-206.

[30] Xue CF, Tu B, Zhao DY. Evaporation-induced coating and self-assembly of ordered mesoporous carbon-silica composite monoliths with macroporous architecture on polyurethane foams. Adv Funct Mater 2008;18(24):3914-21.

[31] Lai C, Gao X, Zhang B, Yan T, Zhou Z. Synthesis and electrochemical performance of sulfur-highly porous carbon composites. J. Phys. Chem. C 2009;113(11): 4712-6.

[32] Ward, AT. Raman spectroscopy of sulfur, sulfur-selenium, and sulfur-arsenic mixtures. J. Phys. Chem. 1968;72(12):4133-9.

[33] Yuan LX, Feng JK, Ai XP, Cao YL, Chen SL, Yang HX. Improved dischargeability and reversibility of sulfur cathode in a novel ionic liquid electrolyte. Electrochem. Commun. 2006;8(4):610-4.

[34]Zhou GM, Wang DW, Li F, Hou PX, Yin LC, Liu C, et al. A flexible nanostructured sulfur-carbon nanotube cathode with high rate performance for Li-S batteries. Energy Environ Sci 2012;5(10):8901-6.

[35] Li GC, Li GR, Ye SH, Gao XP. A polyaniline-coated sulfur/carbon composite with an enhanced high-rate capability as a cathode material for lithium/sulfur batteries. Adv Energy Mater 2012;2(10):1238-45.

[36] Zhang SS. Role of LiNO3 in rechargeable lithium/sulfur battery. Electrochim Acta 2012;70:344-8.

[37] Yuan LX, Qiu XP, Chen LQ, Zhu WT. New insight into the discharge process of sulfur cathode by electrochemical impedance spectroscopy. J Power Sources 2009;189(1):127-132.